Dislodging a sessile drop by a high-Reynolds-number shear flow at subfreezing temperatures

Ilia V. Roisman,* Antonio Criscione,† and Cameron Tropea
Institute for Fluid Mechanics and Aerodynamics, Center of Smart Interfaces, Technische Universtität Darmstadt, D-64287, Germany

Deepak Kumar Mandal and Alidad Amirfazli
Department of Mechanical Engineering, York University, M3J 1P3, Canada
(Received 2 May 2015; published 5 August 2015)

The drop, exposed to an air flow parallel to the substrate, starts to dislodge when the air velocity reaches some threshold value, which depends on the substrate wetting properties and drop volume. In this study the critical air velocity is measured for different drop volumes, on substrates of various wettabilities. The substrate initial temperatures varied between the normal room temperature (24.5 °C) and subfreezing temperatures (−5 °C and −1 °C). The physics of the drop did not change at the subfreezing temperatures of the substrates, which clearly indicates that the drop does not freeze and remains liquid for a relatively long time. During this time solidification is not initiated, neither by the air flow nor by mechanical disturbances. An approximate theoretical model is proposed that allows estimation of the aerodynamic forces acting on the sessile drop. The model is valid for the case when the drop height is of the same order as the thickness of the viscous boundary in the airflow, but the inertial effects are still dominant. Such a situation, relevant to many practical applications, was never modeled before. The theoretical predictions for the critical velocity of drop dislodging agree well with the experimental data for both room temperature and lower temperatures of the substrates.

DOI: 10.1103/PhysRevE.92.023007 PACS number(s): 47.55.D−, 47.55.np, 68.08.Bc, 68.35.Rh

I. INTRODUCTION

Drop motion on a surface is a subject of research for its practical and fundamental importance with regard to many applications: processing industry (e.g., distillation, water management in fuel cells, spray coating, and condensation) [1,2], oil recovery [3–6], cleaning [7], biological applications [8], soiling of vehicles [9], and the avoidance of airframe icing [10,11].

A sessile drop, exposed to an air cross-flow, initially deforms under the action of the aerodynamic stresses. If the aerodynamic force applied to the drop is high enough, the drop starts to move along the substrate. Various parameters may significantly influence the critical conditions for the incipient or lateral motion of a sessile drop, e.g., viscosity of the liquid [5,12] and the volume of the drop, wettability of the substrate (namely the equilibrium contact angle and the hysteresis), and surface morphology [3,12–14].

Prediction of drop deformation and motion is not a trivial three-dimensional problem, which involves a description of motion and pinning of a contact line. Numerical computation of this phenomenon is a rather challenging task [15–22], which usually requires significant CPU resources.

Theoretical models are often based on the force balance, where the estimation of the force produced by the external flow is a most complicated part. Several sophisticated theoretical models have been developed for drop behavior in a shear creeping flow [23,24] or in a uniform inviscid flow disturbed by a drop [25].

In many practical applications, related, for example, to the water management in the car industry or to the airframe icing, the sessile drops are deposited in a near-wall viscous boundary layer produced by a high-velocity air flow. The Reynolds number in such a flow can be rather high. No existing theory or empirical correlation is able to predict a critical velocity of dislodging of a drop of a given volume on a substrate with given wetting. We have checked all the existing models but they usually fail to predict even a correct order of magnitude for this velocity.

The main subject of the present study is a development of an approximate model, which is able to predict the critical air velocity, associated with the incipient motion of a sessile drop on substrates at normal room temperatures and subfreezing temperatures.

II. EXPERIMENTAL METHOD

Experiments for dislodging of a sessile water drop at ambient and subfreezing temperatures were conducted in a wind tunnel producing a uniform air flow. The water drop was placed on the surface of the sample, 3.7 cm downstream from the leading edge of the surface. A high-speed camera was used to capture the side view images of the drop. Substrates of different wettabilities—hydrophobic, superhydrophobic (SHS), and hydrophilic—were investigated. The average downstream Θ_{down} and upstream Θ_{up} contact angles (defined Fig. 1) for all surfaces under airflow conditions are listed in Table I. Drops placed on the cold substrate ($T = -1\,^{\circ}\mathrm{C}$ and $T = -5\,^{\circ}\mathrm{C}$) had an initial temperature of $T_{drop} \approx 0.5\,^{\circ}\mathrm{C}$. Experiments with different volumes of distilled water drops ranging from 5 to 100 μl were carried out. The height of the water drop range between 1.8 mm (5 μl on PMMA) and 4 mm (100 μl on SHS).

The airflow in the wind channel was gradually increased from zero till the moment at which drop started its motion. Figure 2 shows the results of drop dislodging tests on various substrates at room temperature, $T = 24.5\,^{\circ}\mathrm{C}$, and at subfreezing substrate temperature $T = -5\,^{\circ}\mathrm{C}$. The experimentally

*roisman@sla.tu-darmstadt.de
†Present address: New Devices Engineering, Inflator Global Organization, TAKATA Corporation, Aschaffenburg D-63743, Germany.

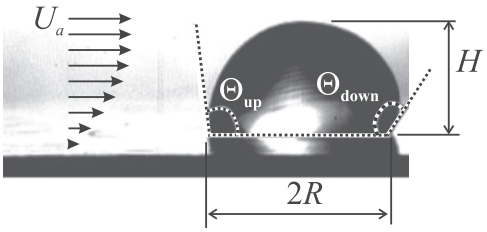

FIG. 1. Side view on a sessile drop, slightly deformed by an air flow.

obtained critical air velocity for incipient motion, U_{crit}, increases as the drop volume, V, decreases. The critical air velocity for the system of water with hydrophilic substrates, i.e., PMMA, are higher than hydro- or superhydrophobic surfaces.

When a drop is placed on a cold substrate, an expanding thermal boundary layer is initiated in both wall and liquid regions. The thickness of the thermal boundary layer in water drop is $h_{thermal} \sim 2\sqrt{\alpha t}$, where α is the thermal diffusivity. The value of thermal diffusivity for distilled water at low temperatures is $\alpha \sim 10^{-7}$ m^2/s. The cooling duration of a millimetric drop, estimated by the moment when the boundary layer thickness is equal to the drop height, is therefore approximately 2–3 s. At longer time the drop temperature can be assumed uniform and equal to the contact temperature [26,27], which is rather close to the initial temperature of a metal wall, whose thermal effusivity is much higher than that of water.

In the experiments the sessile drops cooled to the subfreezing temperatures remain liquid during a relatively long period of time, of the order of minutes (in any case much longer than the typical cooling duration). Neither airflow nor mechanical disturbances by a clean thermocouple trigger solidification. The delay of the solidification of a supercooled drop is determined by the drop size, substrate temperature, morphology, and wettability [28–35].

The delay of solidification explains a relatively weak influence of the temperature on the critical velocity, which can be concluded from the comparison of the results shown in Fig. 2. The main factor responsible for some increase of the critical velocity at subfreezing temperatures is the dependence of the substrates' wettability on temperature [36], Table I.

TABLE I. Downstream and upstream water contact angles at various substrate temperatures.

Surface	T (°C)	Θ_{down} (°)	Θ_{up} (°)	$\cos\Theta_{up} - \cos\Theta_{down}$
PMMA	24.5	88.4 ± 1.6	70.5 ± 5.8	0.31
PMMA	−1	88.8 ± 3.6	69.2 ± 1.1	0.33
PMMA	−5	88.4 ± 2.2	61.6 ± 1.6	0.45
Teflon	24.5	117.4 ± 0.6	107.8 ± 0.9	0.15
Teflon	−1	118.4 ± 1.1	108 ± 1.2	0.17
Teflon	−5	116.7 ± 6.1	96.1 ± 7.1	0.34
SHS	24.5	153.3 ± 2.5	147.1 ± 3.3	0.054
SHS	−1	151.7 ± 2.5	123.6 ± 25	0.33
SHS	−5	148.0 ± 17.8	121.0 ± 5.9	0.33
PDMS	24.5	94.2 ± 5	64 ± 3.2	0.51
PDMS	−1	94.4 ± 2.1	61.2 ± 4.1	0.56
PDMS	−5	100.1 ± 7.5	61.6 ± 6.4	0.65

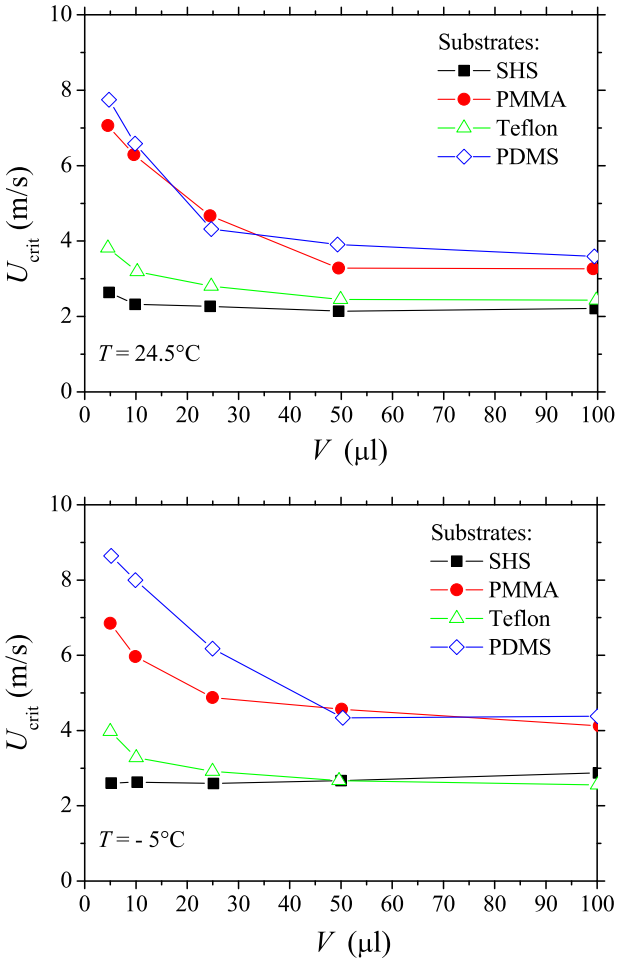

FIG. 2. (Color online) Critical air velocity for drop dislodging, U_{crit}, as a function of the drop volume V, measured at the ambient temperature $T = 24.5\,^{\circ}$C and at the subfreezing substrate temperature $T = -5\,^{\circ}$C. Lines are added for clarity.

III. ESTIMATION OF THE FORCES APPLIED TO THE DROP

The critical air velocity is determined by a balance of the aerodynamic forces applied to the drop and the lateral adhesion force. The expression for the lateral adhesion force is well-known,

$$F_{adh} = w\gamma(\cos\Theta_{up} - \cos\Theta_{down}), \quad (1)$$

where w is the drop width, and γ is the surface tension. Equation (1) is based on the assumption that the contact line consists of four segments: two segments, dewetting and wetting with the contact angles Θ_{up} and Θ_{down}, and two straight segments parallel to the drop motion, where the contact angle is not defined [37]. Equation (1) has been recently confirmed by direct measurements of the lateral adhesion force [38].

One of the parameters determining the aerodynamic force applied to a sessile drop is the ratio of the drop height to the thickness of the near-wall viscous boundary layer in the

air flow. If this ratio is much higher than unity, the effect of the boundary layer can be neglected and the flow around the drop can be approximated by a potential flow with separation, defined by the viscosity [25]. The drag force is defined mainly by the air velocity and drop geometry.

A different situation arises if the height of the drop is of the same order or much smaller than the thickness of the boundary layer. The thickness of the laminar boundary layer can be estimated from the Blasius solution, $\delta \approx 5\sqrt{\nu x/U_a}$, where x is the distance downstream from the start of the boundary layer, and U_a is the velocity of the unperturbed air flow far from the wall. In our experiments the distance is $x = 3.7$ cm. The thickness of the boundary layer at the room temperature ranges between 1.4 mm (at $U_a = 8$ m/s) and 2.5 mm (at $U_a = 2.5$ m/s). These values are of the same order of magnitude as the height of the drops used in the experiments. In this case the governing parameter is not the air velocity but the velocity gradient in the viscous boundary layer, dU/dZ, in the direction normal to the surface (i.e., Z). If the inertial forces in the air flow are negligibly small, the drag force is governed by the viscosity and is estimated as $F_{\text{visc}} \sim \mu V^{2/3} dU/dZ$ [24]. If the inertial forces are dominant, the aerodynamic force can be scaled by $F_{\text{inert}} \sim \rho(dU/dZ)^2 V^{4/3}$.

Since the velocity gradient in the laminar boundary layer can be estimated from the Blasius solution [39] as

$$\frac{dU}{dZ} \approx 0.332\sqrt{\frac{U_a^3}{\nu x}}, \tag{2}$$

the corresponding Reynolds number, defined as the ratio of the inertia dominant and viscous forces ($\text{Re} \equiv F_{\text{inert}}/F_{\text{visc}}$) is

$$\text{Re} = \frac{V^{2/3}}{\nu}\frac{dU}{dZ} = 0.332\frac{V^{2/3}}{\nu^{3/2}}\frac{U_a^{3/2}}{x^{1/2}}. \tag{3}$$

Substitution of known material properties and geometrical parameters of our experiment in Eq. (3) allows to estimate the Reynolds number $\text{Re} \sim 10^3$. The case of inertia dominated aerodynamic force in a viscous boundary layer, applied to a sessile drop, has not been considered yet in the literature despite its high relevance to many practical applications.

Let us consider an asymptotic case $(\Theta_{\text{down}} - \Theta_{\text{up}})/\Theta_{\text{down}} \ll 1$. This assumption is not satisfied for all the substrates (for example, $(\Theta_{\text{down}} - \Theta_{\text{up}})/\Theta_{\text{down}} \approx 0.3$ for PDMS). Nevertheless, it helps to roughly estimate the typical length scales of a sessile drop and typical forces applied to it.

If the size of the drop is smaller than the capillary length, the shape of the drop can be approximated well by a truncated sphere. The wetting characteristics between liquid and substrate are represented here by the average static contact angle, $\Theta \equiv (\Theta_{\text{up}} + \Theta_{\text{down}})/2$. It is assumed that the volume of the drop V and the static contact angle of the sessile drop Θ are given. Thus, a geometrical analysis provides the height H, the radius of the base area R, and the frontal projected area of the truncated sphere A, respectively, as follows:

$$H = \left[\frac{6V\sin^2\frac{\Theta}{2}}{\pi(2+\cos\Theta)}\right]^{1/3}, \quad R = H\cot\frac{\Theta}{2}, \tag{4}$$

$$A = H^2\frac{\Theta - \sin\Theta\cos\Theta}{(1-\cos\Theta)^2}. \tag{5}$$

The characteristic velocity of the air around the drop u can be roughly estimated as $u \approx H/2(dU/dZ)$. The pressure at the drop free surface, estimated from the stationary Bernoulli equation, is $p \approx \rho u^2/2$. An approximate expression for the aerodynamic force is obtained with the help of the relation Eq. (2) in the form

$$F_{\text{aero}} \approx \rho\left(\frac{dU}{dZ}\right)^2\frac{H^2 A}{8}. \tag{6}$$

A drop starts to move when the aerodynamic force reaches the value of the lateral adhesion force. This condition yields the following expression for the critical velocity gradient, estimated by equating the forces defined in Eqs. (1) and (6) and approximating the drop width as $w \approx 2R$:

$$\left(\frac{dU}{dZ}\right)_{\text{crit}} = 4\left[\frac{R\gamma}{\rho H^2 A}(\cos\Theta_{\text{up}} - \cos\Theta_{\text{down}})\right]^{1/2}, \tag{7}$$

i.e., the critical air velocity in the channel, $U_a = U_{\text{crit}}$, corresponding to the initiation of the drop dislodging, is

$$U_{\text{crit}} = 5.25\left[\frac{\gamma\nu}{\rho}\frac{Rx}{H^2 A}(\cos\Theta_{\text{up}} - \cos\Theta_{\text{down}})\right]^{1/3}, \tag{8}$$

which is obtained with the help of Eq. (2).

IV. RESULTS AND DISCUSSION

The expression for the critical velocity gradient Eq. (7) is obtained from the rough estimations of the aerodynamic force at high Reynolds numbers. Nevertheless, as shown in Fig. 3, this expression predicts quantitatively rather well the existing experimental data from Ref. [40] for the critical velocity gradient corresponding to the incipient motion of Pristane and Squalane drops in a water shear flow. One "bad" point in the graph corresponds to relatively small Reynolds number, for which the viscous forces in the surrounding flow, not accounted for in the present estimation, become significant.

It can be shown that for the same operational parameters and the same substrate properties the critical velocity U_{crit} is

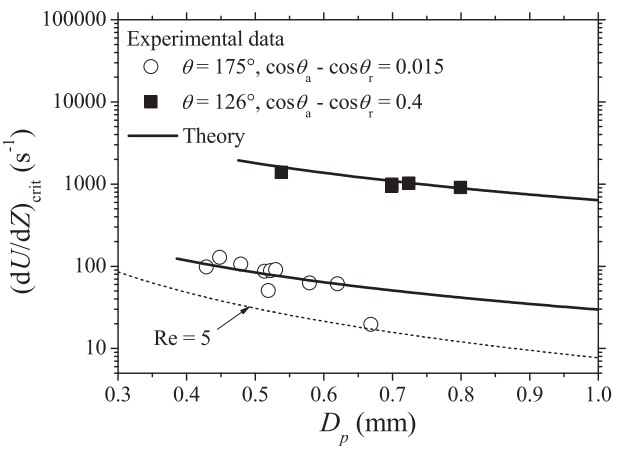

FIG. 3. Critical velocity gradient for drop dislodging as a function of the drop diameter, D_p. The experimental data from Ref. [40] in comparison with the theoretical predictions Eq. (7).

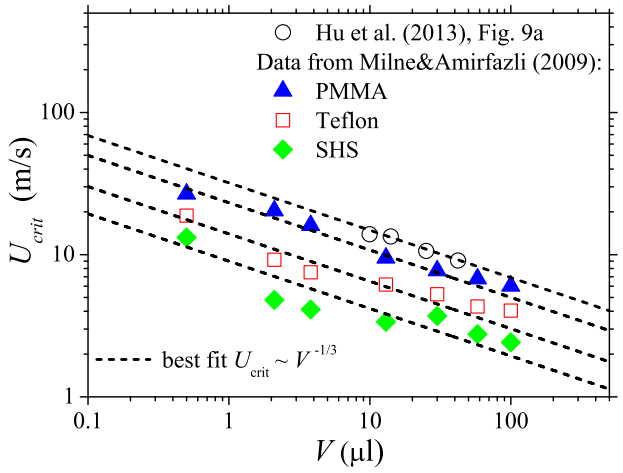

FIG. 4. (Color online) Critical air velocity for drop dislodging, U_{crit}, as a function of the drop volume, V. The experimental data from Refs. [13,14] in comparison with the fit $U_{\text{crit}} \sim V^{-1/3}$.

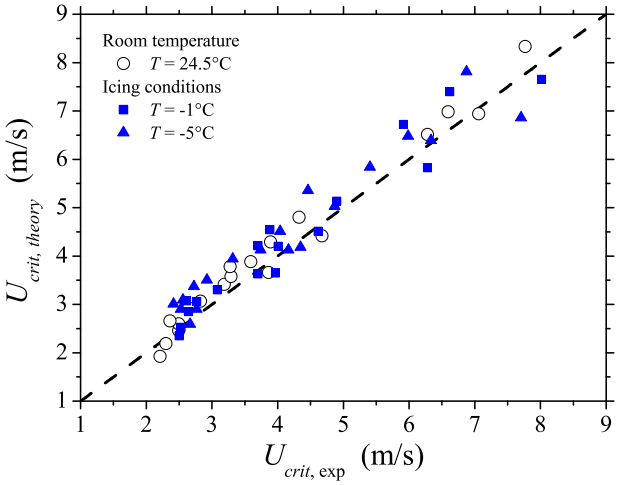

FIG. 5. (Color online) Comparison of the measured critical velocity for drop dislodging $U_{\text{crit,exp}}$, measured in this study, with the theoretical prediction $U_{\text{crit,theory}}$ by Eq. (8).

proportional to $V^{-1/3}$. This relation is confirmed in Fig. 4 by the comparison of the fit $U_{\text{crit}} \sim V^{-1/3}$ with the existing experimental data from Refs. [13,14].

As shown in Fig. 5, our rough prediction for the critical velocity expressed in Eq. (8) agrees excellently with the experimental data. The reason for such good agreement lies in the correct choice of the main factors determining the aerodynamic force, namely the inertia based on the velocity gradient in the viscous boundary layer of the outer air flow.

ACKNOWLEDGMENTS

This research was supported by the Natural Sciences and Engineering Research Council of Canada, and partially CRIAQ, PWC, Bombardier-Canada and by the German Scientific Foundation (Deutsche Forschungsgemeinschaft) in the framework of the SFB-TRR 75 collaborative research center.

[1] P. Dimitrakopoulos and J. Higdon, J. Fluid Mech. **336**, 351 (1997).
[2] V. Cristini and Y.-C. Tan, Lab Chip **4**, 257 (2004).
[3] S. Madani and A. Amirfazli, Colloids Surf. A **441**, 796 (2014).
[4] J. Bear, Ph.D. thesis, Technion-Israel Institute of Technology, Haifa, Israel (1972).
[5] M. Mahe, M. Vignes-Adler, and P. M. J. Adler, J. Colloid Interface Sci. **126**, 329 (1988).
[6] A. Schleizer and R. Bonnecaze, J. Fluid Mech. **383**, 29 (1999).
[7] V. Thoreau, B. Maiki, G. Berthome, L. Boulange-Petermann, and J. Joudi, J. Adhes. Sci. Technol. **20**, 1819 (2006).
[8] S. Hodges and O. Jensen, J. Fluid Mech. **460**, 381 (2002).
[9] T. Hagemeier, M. Hartmann, and D. Thevenin, Int. J. Multiphase Flow **37**, 860 (2011).
[10] T. Theodorsen and W. C. Clay, T.R. 403, N.A.C.A. (1931).
[11] S. Tarquini, C. Antonini, A. Amirfazli, M. Marengo, and J. Palacios, Cold Reg. Sci. Technol. **100**, 50 (2014).
[12] J. Fan, M. Wilson, and N. Kapur, J. Colloid Interface Sci. **356**, 286 (2011).
[13] H. Hu, S. Huang, and L. Chen, Exp. Thermal Fluid Sci. **49**, 86 (2013).
[14] A. J. B. Milne and A. Amirfazli, Langmuir **25**, 14155 (2009).
[15] J. L. Jones, M. Lal, J. N. Ruddock, and N. A. Spenley, Faraday Discuss. **112**, 129 (1999).
[16] S. Yon and C. Pozrikidis, Phys. Fluids **11**, 1297 (1999).
[17] P. Dimitrakopoulos, J. Fluid Mech. **580**, 451 (2007).
[18] M. Ahmadlouydarab and J. J. Feng, J. Fluid Mech. **746**, 214 (2014).
[19] A. K. Gupta and S. Basu, Chem. Eng. Sci. **63**, 5496 (2008).
[20] H. Ding and P. D. Spelt, J. Fluid Mech. **599**, 341 (2008).
[21] H. Ding, M. N. Gilani, and P. D. Spelt, J. Fluid Mech. **644**, 217 (2010).
[22] N. Linder, A. Criscione, I. V. Roisman, H. Marschall, and C. Tropea [Theor. Comp. Fluid Dyn. (to be published)].
[23] M. E. O'Neill, Chem. Eng. Sci. **23**, 1293 (1968).
[24] E. B. Dussan V., J. Fluid Mech. **174**, 381 (1987).
[25] P. A. Durbin, J. Fluid Mech. **196**, 205 (1988).
[26] H. S. Carslaw and J. C. Jaeger, *Conduction of Heat in Solids* (Clarendon Press, Oxford, 1959), 2nd ed.
[27] I. V. Roisman, J. Fluid Mech. **656**, 189 (2010).
[28] G. Tammann and A. Büchner, Z. Anorg. Allg. Chem. **222**, 371 (1935).
[29] E. K. Bigg, Proc. Phys. Soc. B **66**, 688 (1953).
[30] S. Toschev and I. Gutzow, Phys. Status Solidi B **21**, 683 (1967).
[31] P. Tourkine, M. Le Merrer, and D. Quéré, Langmuir **25**, 7214 (2009).
[32] L. Yin, Q. Xia, J. Xue, S. Yang, Q. Wang, and Q. Chen, Appl. Surf. Sci. **256**, 6764 (2010).
[33] D. P. Singh and J. P. Singh, Appl. Phys. Lett. **102**, 243112 (2013).
[34] G. Heydari, E. Thormann, M. Jaärn, E. Tyrode, and P. M. Claesson, J. Phys. Chem. C **117**, 21752 (2013).

[35] L. Boinovich, A. M. Emelyanenko, V. V. Korolev, and A. S. Pashinin, Langmuir **30**, 1659 (2014).
[36] F. Tavakoli and H. P. Kavehpour, Langmuir **31**, 2120 (2015).
[37] E. B. Dussan V. and R. T.-P. Chow, J. Fluid Mech. **137**, 1 (1983).
[38] D. W. Pilat, P. Papadopoulos, D. Schaffel, D. Vollmer, R. Berger, and H.-J. Butt, Langmuir **28**, 16812 (2012).
[39] H. Schlichting, K. Gersten, and K. Gersten, *Boundary-Layer Theory* (Springer, Berlin, 2000).
[40] M. Mahe, M. Vignes-Adler, A. Rousseau, G. Jacquin, and P. M. Adler, J. Colloid Interface Sci. **126**, 314 (1988).